Role of autoionization and characteristic decay in core-electron energy-loss spectra of La and Ce

K. Nuroh*
Department of Mathematical Sciences, Kent State University, Salem, Ohio 44460
(Received 3 July 2002; published 31 October 2002)

A theoretical model is presented for an analytical treatment of electron-impact ionization intensity profiles in the region of an isolated core-electron excitation threshold. Allowing for core-hole lifetime broadening through autoionization and characteristic decay mechanism, Fano line shapes are obtained for $4d \rightarrow 4f$ transitions in La and Ce.

DOI: 10.1103/PhysRevB.66.155126 PACS number(s): 71.27.+a, 71.28.+d, 79.20.Fv, 79.20.Uv

I. INTRODUCTION

Within the last three decades, experimentalists have recognized inelastic electron scattering as one of the best tools for the investigation of the electronic structure of metals and their compounds, particularly at their surfaces. While spectroscopic techniques such as appearance potential spectroscopy, bremsstrahlung isochromat spectroscopy, and electron energy-loss spectroscopy (EELS) derive from such a probe, by far the most preferred technique is EELS. There is certainly no dearth of experimental data in the literature on the EELS technique. In particular, there are extensive EELS measurements near the $3d$-, $4d$-, and $5d$-excitation thresholds for the rare-earth metals,[1–4] and several of such measurements near the $2p$- and $3p$-excitation thresholds for the transition metals.[5–8] As is often the case, theoretical calculations lag behind available experimental data. When such calculations exist, the focus has been on a particular aspect of the overall spectrum. For instance, the resonantlike structures found in experiment have been supported with configuration-interaction calculations within some approximate scheme such as intermediate coupling,[3] LS coupling, or *jK* coupling.[9] In the work of Leapman, Rez, and Mayers,[10] the focus had been mainly on core edge shapes as a function of the momentum transfer of the impinging electron to the scattering system. Moser and Wendin[11] have also performed similar calculations with inclusion of spin-flip components in their formulation. The rudimentary Born approximation is used for the latter two studies.

Apart from the foregoing, the various theoretical formulations geared specifically for EELS, and other formulations that have been used indirectly to interpret EELS, may be grouped into three broad categories, without loss of generality. The first uses the surface or bulk dielectric function for an extended system as the central input.[12–20] The second uses the Fano formalism[21] of discrete state(s) interacting with continuum state(s).[22–26] The third looks at spectral line shapes arising from inner core excitations as a consequence of the correlation between the core hole and the system electrons using perturbation theory.[27] It is generally acknowledged that for high incident electron energies and small scattering angles, EELS is similar to x-ray absorption and to some extent x-ray photoelectron spectra, because the dipole approximation is valid. As a consequence, calculated photoabsorption spectra may be used for comparison with, and interpretation of EELS. Using the Fano formalism, Dehmer, Starace, Fano, Sugar, and Cooper[22–25] calculated the photoabsorption spectra of the lanthanides that compared very well with measurements. It was the success of the above series of work that spurred Davis and Feldkamp to use the Fano formalism to calculate relative EEL absorption cross sections, and to interpret the core-excited spectra of some transition metals in the dipole limit for some transition metals.[26]

The outlined model here is a hybrid between the Fano formalism, the approach of Davis and Feldkamp, and the perturbation treatment used by Schönhammer and Gunnarsson[27] in which the shape of core-level spectra of adsorbates was deduced as a consequence of relaxation effects emanating from the created hole. The approach, however, will use atomic perturbation theory, and more importantly, will not assume the dipole approximation. Rather, the full Coulomb interaction of the incident electron with the system electrons will be used as the transition-matrix element. Taking correlation effects into account, the relevant parameters that enter the Fano line intensity profiles will be calculated. Second, and more significantly, the approach distinguishes between two decay channels—autoionizing and characteristic.

II. FORMULATION

The inelastic scattering of the primary electron of energy E may be viewed as the reaction equation,

$$E + 4d^{10}4f^{N} \rightarrow 4d^{9}4f^{N+1} \rightarrow 4d^{9}4f^{N} + \epsilon, \qquad (1)$$

where $N=0$ for La and $N=1$ for Ce for we consider atomic La and Ce as triply ionized in a metallic environment. In the deexcitation process, the intermediate $4d^{9}4f^{N+1}$ state may decay by two processes. In one case, the d hole may be filled by the excited virtual $4f$ electron, with the ϵ electron being sent into another continuum state. (While there is no $4f$ electron in the ground state of La, there exists an excited bound $4f$ electron below the Fermi level of the metal when a vacancy is created in the inner d shell.[28] It is this $4f$ electron that is described as virtual. In Ce, this $4f$ electron is distinguished from the one that is in the ground state—the valence band, because their wave functions and energies correspond to different ionic potentials.) This flip-flop interaction involving multiple scattering of the impinging electron E constitutes the autoionization decay channel. In the other situation, the d hole may be filled by an occupied $4f$ electron in the

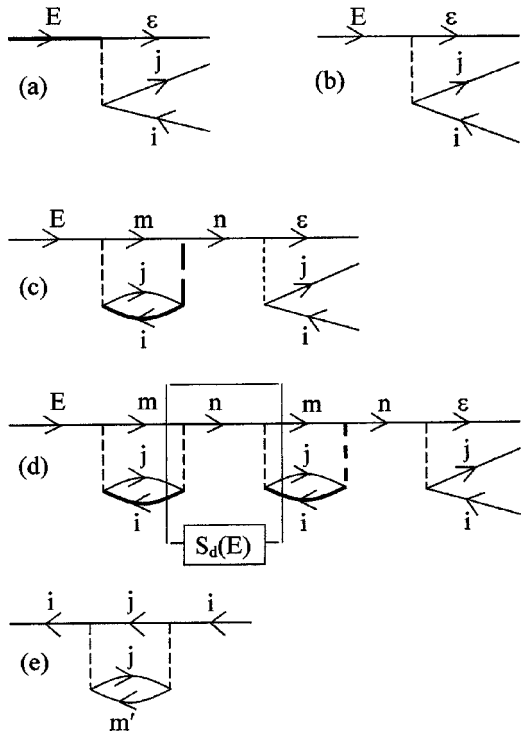

FIG. 1. Perturbative excitation diagrams: (a) the effective excitation amplitude; (b) the nonresonant contribution to (a); (c) the first-order contribution to (a); (d) the second-order contribution to (a); (e) the core-hole self-energy describing characteristic decay amplitude. The assignment for the states are as follows: $i \rightarrow 4d$, $j \rightarrow 4f$, $m \rightarrow nf$, $\epsilon \rightarrow \epsilon f$, $E \rightarrow Eg$, $m' \rightarrow ng$.

valence band, while another $4f$ electron is sent into the continuum. This type of interaction constitutes the characteristic decay channel. We use the descriptive term characteristic here in the sense of the lifetime broadening associated with a vacancy in an inner shell. Taking these types of interaction processes to infinite order is equivalent to representing the wave function for the state $|E\rangle$ by an effective one in the Coulomb excitation amplitude. In doing so, we may view the pseudodiscrete state $4d^9 4f^{N+1}$ as interacting with the continuum level $4d^9 4f^N \epsilon l$, and the Fano autoionization parameters may be introduced when the square of the absolute value of the Coulomb excitation amplitude is taken to give the scattering cross section. The picture here must, however, be distinguished from an atomic calculation of the contribution of inner-shell excitation followed by autoionization to ionization including interference effects via the Fano formalism.[21–25]

First, the EELS technique samples a veneer of atoms at the surface of the metal. Second, the $4d \rightarrow 4f$ excitation is a localized one. Hence, an atomic picture description is justified for an otherwise itinerant solid-state problem. Thus, using diagrammatic atomic perturbation theory, the effective excitation amplitude is represented by Fig. 1(a), where the thick line on the propagator for the E state denotes a renormalized one. Figure 1(b) represents the nonresonant contribution of the excitation amplitude, and is denoted by the interaction matrix element $V_{\epsilon E}$. Figure 1(c) represents the first-order contribution to (a). It introduces the discrete state and intermediate Coulomb interaction parameter V_{nd}, and the discrete state and the primary electron Coulomb interaction V_{dE}. Figure 1(d) represents the second-order contribution to (a) and introduces an irreducible self-energy of the discrete state, $S_d(E)$,[29] describing the autoionizing flip-flop processes. Some aspects of the model are similar to those presented in the discussion of atomic and solid-state effects in threshold $3p$ emission in transition metals.[30] If all higher-order contributions are included to describe the renormalized propagator of Fig. 1(a), we would retain the basic diagrams in Figs. 1(b)–1(d), except that the i-hole propagator will have to be replaced by its self energy, $\Sigma_d(E)$, which represents the characteristic decay processes. This is denoted by the thick dashed i line and Fig. 1(e) represents this self energy. Also the interaction V_{nd} has to be replaced by an effective one $V_d(E)$, between the pseudodiscrete state and the continuum level, and is denoted by the thick dashed vertical line. The designation of the various state labels in Figs. 1(a)–1(e) are as indicated in the figure caption. Taking the diagrams of Figs. 1(b), 1(c), and 1(d) plus all higher-order contributions generates an infinite series for the excitation amplitude $a(E)$ given by

$$a(E) = V_{\epsilon E} + V_{\epsilon n} \frac{V_d(E)}{E_d - E} V_{dE} + V_{\epsilon n} \frac{V_d(E)}{E_d - E} \frac{[S_d(E) + \Sigma_d(E)]}{E_d - E} V_{dE} + \cdots, \quad (2)$$

where the energy dependent complex quantities that enter Eq. (2) above are given by

$$V_d(E) = \sum_n \frac{V_{nd}}{E_n - E - i\delta} = \sum_n{}' \frac{V_{nd}}{E_n - E} + i\pi V_{Ed} \delta(E_n - E), \quad (3)$$

$$S_d(E) = \sum_n \frac{V_{nd}^2}{E_n - E - i\delta} = \sum_n{}' \frac{V_{nd}^2}{E_n - E} + i\pi V_{Ed}^2 \delta(E_n - E), \quad (4)$$

$$\Sigma_d(E) = \sum_n \frac{V_n^2}{E_n - E - i\delta} = \sum_n{}' \frac{V_n^2}{E_n - E} + i\pi V_E^2 \delta(E_n - E), \quad (5)$$

with $E_d = (E_m + E_j - E_i) + (E_{m'} - E_j - E_j)$, and the prime on the summation sign signifies principal part summation over discrete states and/or integration over the continuum states. The Fano asymmetry parameter $q(E)$ and the energy parameter $\eta(E)$ are introduced via the effective interaction and the self energies, respectively, as

$$q = -\frac{\mathrm{Re}\, V_d(E)}{\mathrm{Im}\, V_d(E)}, \quad \eta = \frac{\mathrm{Re}\{E - E_d + S_d(E) + \Sigma_d(E)\}}{\mathrm{Im}\{E - E_d + S_d(E) + \Sigma_d(E)\}}. \quad (6)$$

Inserting Eqs. (3)–(6) in Eq. (1) casts the excitation amplitude in the simpler form

$$a(E) = V_{\epsilon E}\{1 + (\Gamma_a / \Gamma_t)[(q - i)/(\eta + i)]\}, \quad (7)$$

where the full width parameters for autoionization Γ_a, for the characteristic decay Γ_c, and the total width Γ_t are defined, respectively, as

$$\Gamma_a = 2\pi V_{Ed}^2, \quad \Gamma_c = 2\pi V_E^2, \quad \Gamma_t = \Gamma_a + \Gamma_c . \tag{8}$$

The differential scattering intensity per unit energy is proportional to the absolute value squared of the excitation amplitude, that is, $dI(E)/dE \sim |a(E)|^2$. Hence we get, using Eq. (7),

$$\frac{dI(E)}{dE} \sim V_{\epsilon E}^2 \left\{ \left[1 + \frac{\Gamma_a}{\Gamma_t} \left(\frac{\eta q - 1}{\eta^2 + 1} \right) \right]^2 + \left(\frac{\Gamma_a}{\Gamma_t} \right)^2 \frac{(\eta + q)^2}{(\eta^2 + 1)^2} \right\}. \tag{9}$$

In applying the formalism to the La and Ce, it is taken that the atom in the metallic environment is triply ionized. For La, this means that we have to set Γ_c to zero because the characteristic channel would make no contribution. This is equivalent to setting $\Gamma_a/\Gamma_t = 1$ in Eq. (9) to obtain the differential scattering intensity under this condition to be

$$dI(E)/dE \sim V_{\epsilon E}^2 (\eta + q)^2/(\eta^2 + 1). \tag{10}$$

Equation (10) is essentially the Fano line profile while Eq. (9) is a modified Fano line profile in the presence of characteristic events. In order to apply Eqs. (9) and (10) to the systems under consideration, explicit expressions are required for the interaction matrix elements V_{nd}^2, V_n^2, and $V_{\epsilon E}$. From the diagram for the irreducible self energy $S_d(E)$, we obtain

$$\begin{aligned} V_{nd}^2 = {} & \frac{44}{49} R^1(\cdot)^2 + \frac{60}{539} R^3(\cdot)^2 + \frac{8100}{121\,121} R^5(\cdot)^2 \\ & - \frac{8}{49} R^1(\cdot) R^3(\cdot) - \frac{40}{539} R^1(\cdot) R^5(\cdot) \\ & - \frac{240}{5929} R^3(\cdot) R^5(\cdot), \end{aligned} \tag{11}$$

where $(\cdot) = (i, E; j, m)$. Here and in what follows, the orbital assignments are as follows: $i \to 4d$, $j \to 4f$, $m \to nf$, $\epsilon \to \epsilon f$, $E \to Eg$, and $m' \to ng$. From the diagram for the self-energy $\Sigma_d(E)$, we obtain

$$\begin{aligned} V_n^2 = {} & \frac{44}{35} R^1(\cdot)^2 + \frac{12}{77} R^3(\cdot)^2 + \frac{8100}{121\,121} R^5(\cdot)^2 \\ & - \frac{8}{35} R^1(\cdot) R^3(\cdot) - \frac{8}{77} R^1(\cdot) R^5(\cdot) - \frac{48}{847} R^3(\cdot) R^5(\cdot), \end{aligned} \tag{12}$$

with $(\cdot) = (i, m'; j, j)$. Finally, for the excitation matrix element, from Fig. 1(b), we have for the $d \to f$ transitions in the lanthanides,

$$V_{\epsilon E} = 2\sqrt{3} R^1(\cdot) + 2(\sqrt{66}/11) R^3(\cdot) + 10(\sqrt{390}/143) R^5(\cdot), \tag{13}$$

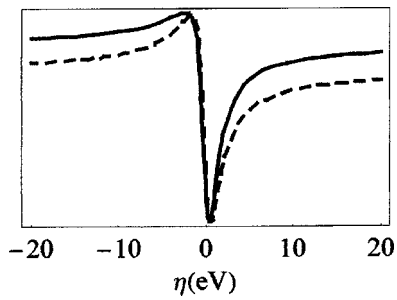

FIG. 2. The calculated $4d$-core-excitation Fano spectral profiles for La and Ce. Solid line, Ce; dashed line, La.

with $(\cdot) = (\epsilon, j; E, i)$. In Eqs. (11)–(13), the R^k $(k = 1,3,5)$ represent the Slater integrals. We note in passing that the angular factors that appear in Eq. (13) are used in determining V_{Ed} in Eq. (3).

The sign associated with the Fano asymmetric parameter q is crucial in determining whether the spectral-like line shape has the feature of a height-to-dip $(q < 0)$, or a dip-to-height $(q > 0)$. In Eq. (6), $\mathrm{Re}\, V_d(E)$ involves a principal part integration of the integrand $|V_{nd}(E)|$ which is a slowly varying function. Assuming this to be a constant function in the vicinity of the excitation edge, the principal part integration yields a value $\sim \ln|(E_0 - \Delta)/E_0| < 0$. Here Δ is the multiplet width of the $nd^9 4f^{N+1}$ configuration and E_0 is the $nd \to 4f$ resonance energy. [The assumption of linear dependence of $|V_{nd}(E)|$ on E that reflects the real situation leads to the same conclusion that $\mathrm{Re}\, V_d(E_0)$ is negative.] Consequently, the sign of the asymmetry parameter q is solely determined by the interaction matrix element V_{Ed}, which in turn determines $\mathrm{Im}\, V_d(E)$ in Eq. (6). From Eq. (13), we find that $V_{Ed} \sim R^k(E, i; m, j)$. The signs of these Slater integrals are determined by the radial overlap integrals $R^k(i,j) = \langle i | r^k | j \rangle$. For the lanthanides, $R^k(4d, 4f) < 0$ and hence $q < 0$, while $R^k(3d, 4f) > 0$ and hence $q > 0$. Taking the full energy dependence into account, the following values were found for q: for $3d \to 4f$ transitions, $q = 0.361$ for La and $q = 0.491$ for Ce; for $4d \to 4f$ transitions, $q = -0.609$ for La and $q = -0.780$ for Ce. The important conclusion here is that the signs associated with the q values are opposite for the $3d \to 4f$ and $4d \to 4f$ transitions in the lanthanides. This distinction is especially important if and when the Fano line profile formula is to be used phenomenologically in conjunction with measurements. The continuum state functions used in these computations have been determined using spherically averaged Hartree-Fock localized potential with a hole in the relevant core subshell of the atom. The ratios of the autoionizing widths to the total widths, Γ_a/Γ_t, as defined via Eqs. (5), (6), and (8) have been computed to be 0.322 for the $4d \to 4f$ transition in Ce.

III. RESULTS AND DISCUSSION

With the above numerical values, the relative EELS for the $4d \to 4f$ transitions in Ce and La have been calculated using Eqs. (9) and (10), respectively, without the inclusion of the excitation interaction $V_{\epsilon E}^2$. This is displayed in Fig. 2,

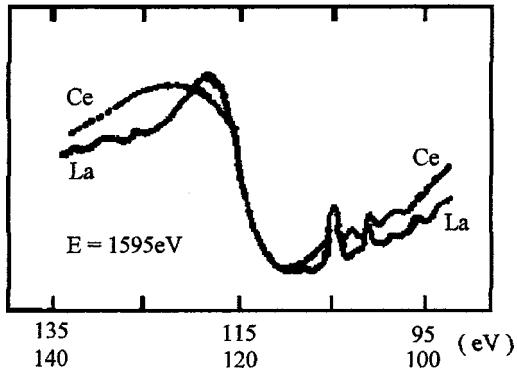

FIG. 3. Relative energy-loss measurements of La and Ce from Ref. 2(a). The upper scale is for La.

while Fig. 3 is the corresponding experimental data from Ref. 2(a) recorded for $E=1595$ eV. In the presentation of the experimental data, the discussion is mute on the normalization of the relative intensities. However, a cursory look at the data for La and Ce suggests that their peak-to-dip heights have been normalized. For this reason the theoretical peak-to-dip heights have been normalized. In comparing theory with experiment, it is more meaningful to rigidly shift the energy scales in order to superimpose the experimental data on one another so that their heights are aligned. The present formulation does not incorporate spin-orbit interaction that is responsible for the discrete sharp structures found in experiment. However, their origin is well understood from multiplet calculations.[9,25] Excluding these effects we find an overall very good agreement between theory and experiment. In particular, we note that the experimental giant resonance is broader and smoother in Ce than in La—and theory reflects these features as well. As is typical in such atomic-based calculations,[9(b),28] the theoretical dips are deeper than those found in experiment. Perhaps the shortcoming of the model presented here compared with the configuration interaction calculations[22–25] is that the theoretical line widths are a few eV smaller than what is found in experiment. We note in passing that the calculated Γ_t for La is 1.4 eV. This value is the same as one of the measured values cited in Ref. 2(a), and that was used as one of the input parameters for the calculated $3d \rightarrow 4f$ EELS for La,[9(b)] when spin-orbit interaction was incorporated via *jK* coupling to discuss the dynamic effects associated with EELS measurements in Ref. 1. In conclusion, the separation of decay events into autoionizing and characteristic channels following an electron-impact excitation of an inner-shell electron provides an alternative perspective for analyzing electron energy-loss spectra using the Fano formalism.

ACKNOWLEDGMENTS

I wish to acknowledge insightful discussions with G. Wendin. This work has been partially supported by IAEA (Vienna), the Swedish Institute and Kent State University's Research Council.

*Email address: nuroh@salem.kent.edu

[1] J. Kanski and G. Wendin, Phys. Rev. B **24**, 4977 (1981).
[2] (a) J. A. D. Matthew, G. Strasser, and F. P. Netzer, Phys. Rev. B **27**, 5839 (1983); (b) F. P. Netzer, G. Strasser, and J. A. D. Matthew, Phys. Rev. Lett. **51**, 211 (1983); (c) Solid State Commun. **45**, 171 (1983); (d) G. Strasser, G. Rosina, J. A. D. Matthew, and F. P. Netzer, J. Phys. F: Met. Phys. **15**, 739 (1985).
[3] H. R. Moser, B. Delley, W. D. Schneider, and Y. Baer, Phys. Rev. B **29**, 2947 (1984).
[4] F. Della Valle and S. Modesti, Phys. Rev. B **40**, 933 (1989).
[5] M. De Crescenzi, F. Antonangeli, C. Bellini, and R. Rosei, Phys. Rev. Lett. **50**, 1949 (1983); Solid State Commun. **46**, 875 (1983); M. De Crescenzi, G. Chiarello, E. Colvaita, and R. Memeo, Phys. Rev. B **29**, 3730 (1984); M. De Crescenzi, G. Chiarello, E. Colavita, and R. Rosei, Solid State Commun. **44**, 845 (1982); M. De Crescenzi and G. Chiarello, J. Phys. C **18**, 3595 (1985).
[6] R. E. Dietz, E. G. McRae, and J. H. Weaver, Phys. Rev. B **21**, 2229 (1980).
[7] L. Lozzi, M. Passacantando, P. Picozzi, S. Santucci, M. Diociaiuti, and M. De Crescenzi, Solid State Commun. **83**, 921 (1992).
[8] M. B. Stearns, L. A. Feldkamp, and S. S. Shinozaki, Bull. Am. Phys. Soc. **20**, 358 (1972).
[9] (a) K. Nuroh, Solid State Commun. **85**, 61 (1993); (b) Phys. Scr. **61**, 589 (2000).
[10] R. D. Leapman, P. Rez, and D. F. Mayers, J. Chem. Phys. **72**, 1232 (1980).
[11] H. R. Moser and G. Wendin, Phys. Rev. B **44**, 6044 (1991).
[12] T. Jach and S. M. Girvin, Phys. Rev. B **27**, 9 (1983).
[13] S. Modesti, F. Della Valle, C. J. Bocchetta, E. Tossati, and G. Paolucci, Phys. Rev. B **36**, 4503 (1987).
[14] J. M. Auerhammer and P. Rez, Phys. Rev. B **40**, 2024 (1989).
[15] Xudong Weng, P. Rez, and O. F. Sankey, Phys. Rev. B **40**, 5694 (1989).
[16] D. K. Saldin and Y. Ueda, Phys. Rev. B **46**, 5100 (1992); Y. Ueda and D. K. Saldin, *ibid.* **46**, 13 697 (1992).
[17] F. Yubero, J. M. Sanz, B. Ramskov, and S. Tougaard, Phys. Rev. B **53**, 9719 (1996).
[18] R. Fuchs, R. G. Barrera, and J. L. Carrillo, Phys. Rev. B **54**, 12 824 (1996).
[19] Y. F. Chen, Phys. Rev. B **58**, 8087 (1998).
[20] I. O. Sosa, C. I. Mendoza, and R. G. Barrera, Phys. Rev. B **63**, 144201 (2001).
[21] U. Fano, Phys. Rev. **124**, 1866 (1961).
[22] T. F. O'Malley and S. Geltman, Phys. Rev. **137**, A1344 (1965).
[23] J. L. Dehmer, A. F. Starace, U. Fano, J. Sugar, and J. W. Cooper, Phys. Rev. Lett. **26**, 1521 (1971).
[24] A. F. Starace, Phys. Rev. B **5**, 1773 (1972); J. Phys. B **7**, 14 (1974).
[25] J. Sugar, Phys. Rev. B **5**, 1785 (1972).
[26] L. C. Davis and L. A. Feldkamp, Solid State Commun. **19**, 413 (1976); Phys. Rev. A **17**, 2012 (1978).
[27] K. Schönhammer and O. Gunnarsson, Solid State Commun. **26**, 399 (1978); O. Gunnarsson and K. Schönhammer, Phys. Rev. Lett. **50**, 604 (1983).
[28] G. Wendin and K. Nuroh, Phys. Rev. Lett. **39**, 48 (1977).
[29] G. Wendin, J. Phys. B **3**, 455 (1970).
[30] G. Wendin and K. Nuroh, Bull. Am. Phys. Soc. **24**, 367 (1979); **24**, 506 (1979).